

Resonant second-harmonic generation in type-II heterostructures of $\text{InP}/\text{Al}_{0.48}\text{In}_{0.52}\text{As}$

F. Bogani and S. Cioncolini

Dipartimento di Fisica and European Laboratory for Non-linear Spectroscopy, Largo Enrico Fermi 2, 50125 Firenze, Italy

E. Lugagne-Delpon, Ph. Roussignol, and P. Voisin

Laboratoire de Physique de la Matière Condensée de l'Ecole Normale Supérieure, 24 rue Lhomond, 75005 Paris, France

J. P. André

Laboratoire d'Electronique Philips, 22 Avenue Descartes, 94453 Limeil-Brévannes Cedex, France

(Received 27 December 1993)

We report an experimental study of the second-harmonic generation in a type-II $\text{InP}/\text{Al}_{0.48}\text{In}_{0.52}\text{As}$ heterostructure at frequencies of the fundamental beam resonant with the spatially indirect-band-gap transitions. From the comparison between the second-harmonic spectrum of the heterostructure and that of an InP crystal in the region 1.15–1.45 eV, we show an enhancement of the second-order susceptibility in the former that is related to the transitions between electron- and hole-confined states. From a study of the dependence of the second-harmonic generation on the polarization directions and the sample orientation, the symmetry properties of the second-harmonic tensor have been derived. These correspond to a T_d (bulklike) symmetry class and the data show the predominance, in the visible region, of the contributions to the second-order nonlinear susceptibility coming from transitions involving high-energy nonconfined states. The terms of lower symmetry involving only low-energy confined states give in this case a negligible contribution.

INTRODUCTION

Nonlinear mixing of optical frequencies and linear electro-optic effects are of great practical interest in optical communications and integrated optics. Both effects are related to optical second-order nonlinearities, and recently have been investigated extensively in asymmetric or biased quantum wells (QW's) in order to produce optical nonlinear devices and optical modulators.^{1–11} The basic idea is that asymmetry produces a localization of the electrons and holes at different sites of the heterostructure and gives rise to large of “giant” dipole moments which result in an enhancement of the optical nonlinearities.^{1,11} The enhancement of the second-harmonic coefficient in multiple quantum wells (MQW's) has been obtained through band-gap engineering and compositionally asymmetric structures, and has been reported by several groups. Most of the work has been performed in the IR, also taking advantage of the multiple resonances between subbands;^{3,4,9} only a few works deal with second-harmonic generation in the visible.^{6–8,10} Also, until now, both the experimental and theoretical works dealt mainly with devices based on type-I QW's, where charge separation and asymmetry in the structure is obtained either by means of an electric field or by composition.

Heterostructures of type II, in this respect, can offer interesting advantages as they intrinsically provide charge separation and large dipole moments. Optical nonlinearities in type-II GaAs/AlAs QW's have been investigated,¹² but second-order effects have received attention only very recently.¹⁰

Type-II InP/InAlAs QW's offer attractive characteris-

tics for the realization of optical modulators and nonlinear materials: the electrons are localized in InP and the holes in $\text{Al}_{1-x}\text{In}_x\text{As}$, giving rise to strong longitudinal electric fields and large dipole moments.^{13,14} At the same time their radiative recombination probability is relatively large,¹⁵ indicating a relevant spatial overlap of the confined electron and hole wave functions and a direct (in \mathbf{k} space) radiative transition. In addition, as the recombination energy is lower than the gap energy of the component materials, they offer, in addition to a low absorption at the fundamental frequency, the interesting opportunity of studying the contribution of a specific transition to the nonlinear second-order susceptibility. For these reasons this kind of heterostructure has recently attracted growing attention, and interesting properties, such as quantum photovoltaic effects¹³ and low lasing thresholds, have been experimentally demonstrated.¹⁶

In this paper we report an experimental study of the second-harmonic coefficients in a MQW consisting of alternating layers of InP and $\text{Al}_{1-x}\text{In}_x\text{As}$. The optical and luminescence properties of such a heterostructure have been reported recently, and basic information about the density of states and the radiative transition probability are available.^{15–17} The paper is organized as follows: we start with a general introduction to the resonant second-harmonic generation in semiconductors, with particular attention to the origin of the second-order nonlinearities in type-II QW's. Then we present the experimental set up and then the experimental results obtained for bulk InP and InP-based MQW structures; from a comparison of these results the contribution of the spatially indirect transitions to second-order susceptibility is proved.

GENERAL THEORY

A phenomenological description of second-harmonic generation in semiconductors, with an incident electric field in resonance with states near the band gap, has been developed in the past following several equivalent approaches¹⁸⁻²⁴ to which we shall refer.

Since in the samples under study the excitonic effects are negligible, in the following we shall consider only free charges eventually confined in the wells; if necessary, excitonic contributions can be included in a similar way.

$$\epsilon_0 \chi_{ijk}^{(2)}(2\omega, \omega) = a_{ijk}(2\omega, \omega) + \sum_l \int \frac{d^3k b_{ijk}^l(2\omega, \omega, \mathbf{k}) [1 - n(k) - p(k)]}{\Omega_{eh}^l(k) - \omega - \frac{i}{T_2}} \quad (2)$$

In (2) the second-order susceptibility is written as the sum of a nonresonant part a_{ijk} and a near-resonant contribution related, in our case, to interband transitions of energy $\Omega_{eh}^l(k)$. The index l labels the different transitions between levels, $n(k)$ and $p(k)$ are their occupation numbers, k is the wave vector of the electron and hole forming the pair, and T_2 their dephasing time; the elements a and b of the tensor are complex functions of the frequency ω and include the local-field correction.¹⁹ The occupation numbers n and p in (2) are usually omitted, but, with a resonant excitation, band-filling effects cannot be neglected *a priori*.

The fields involved in the second-harmonic generation, E_1 at the fundamental frequency ω_1 , and E_2 at the frequency $\omega_2 = 2\omega_1$, satisfy the usual Maxwell equations for nonlinear media which can easily be solved in the case of negligible depletion of the incident beam;¹⁹ the explicit solution requires specification of the polarizations and geometry of the incident beams, and in the following we will restrict ourselves to a specific situation of frequent use. We assume that the nonlinear medium has a symmetry T_d (43 m) or D_{2d} (42 m) and a crystallographic axis coincident with the normal to the surface \mathbf{n} . The incident

A correlated e - h pair near the band edge gives rise, in addition to a linear polarization, to a second-order macroscopic polarization $P^{(2)}(\mathbf{R})$ defined by the χ_{ijk} elements of the second-order susceptibility through the relation

$$P_i^{(2)}(\mathbf{R}, 2\omega) = \epsilon_0 \chi_{ijk}^{(2)}(2\omega, \omega) E_j(\mathbf{R}, \omega) E_k(\mathbf{R}, \omega), \quad (1)$$

where \mathbf{R} is a positional coordinate and $E_{j,k}$ the component of the electric field at frequency ω . According to usual expressions, we have

field in the vacuum, represented as a monochromatic plane wave, can be specified completely by the wave vector k_{1v} , the angle of incidence ϑ_{in} , the amplitude E_{1o} , and the polarization direction forming an angle φ with respect to the normal to the plane of incidence. The electric field and the wave vector k_1 inside the sample are completely determined by the Fresnel relations for an absorbing medium with a complex dielectric constant. The second-harmonic field E_2 consists of forward and backward propagating waves at ω_2 ; the latter propagates in the vacuum collinear with the reflected wave at frequency ω_1 . In our case both waves can be detected but, in order to minimize the signal from the substrate, it is more convenient to detect the reflected second-harmonic wave. In many experiments we used a specific configuration with the crystal axes coincident with the reference axes x, y, z ($z \parallel n$), x and z in the incidence plane, the polarization vector of E_1 in this plane, and an incidence angle, in vacuum, $\vartheta_{in} \leq 45^\circ$ (corresponding to an angle inside the sample $\vartheta_T \leq 12^\circ$). In this case the intensity, in the vacuum, of the reflected second-harmonic field, polarized along y , is given by

$$I_{vy} = \frac{8}{\epsilon_0 c} \frac{|\chi_{xyz}^{(2)}|^2}{\{[(n_2 + n_1)\cos(\vartheta_T)]^2 + (\kappa_2 + \kappa_1)^2\} \{[\cos(\vartheta_v) + n_2 \cos(\vartheta_T)]^2 + \kappa_2^2\}} \times \frac{[\sin(\vartheta_v)\cos^2(\vartheta_v)]^2}{n_1^2 + \kappa_1^2} \frac{I_1^2}{\{[1 + n_1 \cos(\vartheta_v)]^2 + [\kappa_1 \cos(\vartheta_v)]^2\}^2}, \quad (3)$$

where n_i (κ_i) is the refractive index (absorbance) at the fundamental ($i=1$) or second harmonic ($i=2$) frequency; I_1 is the intensity of the incident beam; ϑ_v is the angle of the harmonic beam with respect to \mathbf{n} , in vacuum; and we have assumed the angles of the beams at ω and 2ω are equal to ϑ_T inside the sample.

The second-harmonic intensity exhibits, as a function of the photon energy, a variation related to the dispersion

of the second-order susceptibility and of the refractive index and absorbance. In reflection geometry the dependence of the denominator of (3) on ω is smooth, so that the main contribution to this variation arises from $\chi^{(2)}$.

Let us look more closely at the structure of the second-order nonlinear susceptibility, for which various calculations for bulk semiconductors²¹⁻²⁴ and heterostructures have been reported.¹⁻¹¹ We shall distinguish,

in our type-II QW's, two contributions to $\chi^{(2)}$: the first one derives from conduction and valence states inside the same layer (InP of $\text{Al}_{1-x}\text{In}_x\text{As}$ in our case) and is not too different from that which we find in a bulk semiconductor; the other contribution is specific of type-II hetero-

structures, and is connected to transitions between states localized at different sites, i.e. electronic states in InP and valence states in $\text{Al}_{1-x}\text{In}_x\text{As}$. The contribution to $\chi^{(2)}$ from only confined states has been calculated for type-I heterostructures,^{1,2} and looks like

$$\chi_{ijk}^{(2)}(\omega_1, \omega_2) = \frac{Ne^3}{2\epsilon_0\hbar^2} \sum_p \sum_{b_1, b_2, b_3} \sum_{l, m, n} f_{b_1, l} \sum_{k_{\parallel}} \frac{\langle \phi_{1, l}^* | r_i | \phi_{2, m} \rangle \langle \phi_{2, m}^* | r_j | \phi_{3, n} \rangle \langle \phi_{3, n}^* | r_k | \phi_{1, l} \rangle}{[\omega_{b_2, m}(\mathbf{k}_{\parallel}) - \omega_{b_1, l}(\mathbf{k}_{\parallel}) - \omega_1 - \omega_2][\omega_{b_3, n}(\mathbf{k}_{\parallel}) - \omega_{b_1, l}(\mathbf{k}_{\parallel}) - \omega_2]}, \quad (4)$$

where N is the number of quantum wells per unit length, $f_{b_1, l}$ is the Fermi function of the ground state $\phi_{1, l}$; $\phi_{2, 3}$ are the wave functions of the confined states, labeled by the band and sublevel indices b and m , with energy $\hbar\omega_{b, m}(\mathbf{k}_{\parallel})$; and \sum_p is the summation over the terms obtained by the proper permutations.¹

All these calculations^{1,5} take into account only transitions, real or virtual, between confined states and, as stated in Ref. 1, only the elements χ_{xxx} , χ_{zxx} , and equivalents are different from zero. This assertion is based on selection rules for transitions between confined levels, and on the cancellation between contributions related to states with different spin orientation.^{1,2} For type-II heterostructures a similar expression and similar conclusions can be retained, with the only difference being that now the confined valence and conduction states belong to different materials and layers. Then in a three-level model for $\chi^{(2)}$ we can take into account a term, labeled χ_C , with a representation like (4), where all indices m refer exclusively to confined states of the conduction or valence bands located in adjacent layers; a schematic picture of the transitions involved in this term is given in Fig. 1(c). The matrix elements appearing in (4) involve transitions, real or virtual, between confined states, and conclusions about the symmetry properties of $\chi^{(2)}$, as well most of the considerations done in Refs. 1 and 2 for type-I heterostructures, can be retained for χ_C . However as it is rather limiting to neglect all the other states, in addition to these contributions to $\chi^{(2)}$, we must consider those where all involved levels belong to the same layer, and those which involve levels between confined and unconfined states in different materials. We shall label the former contribution χ_B , and the latter χ_A ; the three levels and the transitions involved in each term are shown schematically in Figs. 1(b) and 1(a), respectively. For both χ_A and χ_B the element χ_{xyz} is different from zero, and is expected to make the main contribution; an expression like (4) still holds, but in this case at least one pair of indices (b, m) refers to states lying in the continuum. The first term χ_B can have one-photon resonances at energies around those of the direct transitions inside each component material; the second one χ_A , on the contrary, can have one-photon resonances at energies around the indirect band gap; and both terms can have two-photon resonances, as shown by (4). In general a quantitative calculation of second-order susceptibility requires a detailed knowledge of the electronic wave functions and

states and is beyond the aim of the present paper; nevertheless we can obtain some qualitative results about this quantity and the matrix elements appearing in (4). In bulk semiconductors the dispersion of $\chi^{(2)}$ near the band gap is determined mainly by so-called "two-photon resonances" corresponding to the matching of 2ω , with the energy of a transition; for InP, for example, recent calculations²³ show that, in this region, $\chi^{(2)}$ is essentially imaginary and associated with the density of states at frequency 2ω , the one-photon resonances making only a minor contribution. The term χ_B will be essentially the same as that of the bulk semiconductor since, for heterostructures, only minor changes in the dispersion of $\chi^{(2)}$ must be expected from confinement. In other words, in (2), for photon energy near that of the indirect band gap, the main contribution to χ_B comes from the product of the imaginary part of b_{ijk} , related to two-photon resonances, with the real part of the resonant Lorentzian.

More attention is required by the term χ_A , involving

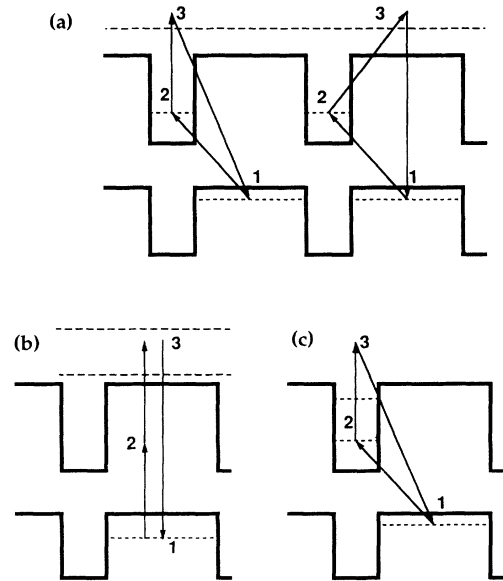


FIG. 1. Schematic picture of the transitions and levels appearing in the terms of the second-order susceptibility. (a) Transitions involving confined and unconfined states in different layers, giving rise to χ_A . (b) Intralayer transitions to be considered in the term χ_B , for one layer. (c) Transitions involving only confined states included in χ_C .

transitions such as those depicted in Fig. 1(a): two of the levels to be taken into account correspond to confined states, in the conduction and valence bands, but the third, unlike that for χ_C , corresponds to an unconfined state of the valence or conduction bands. In this case it results from (4) that one of the matrix elements refers to intraband transitions, the others to interband transitions. One of these necessarily involves a transition between conduction and valence states confined in different layers, and depends on the overlap integral of the electron and hole wave functions appearing in the dipole moment matrix element of the linear susceptibility. The other two matrix elements involve transitions between confined and unconfined states: one, between states in different layers, depends on the penetration of the wave functions in the adjacent material, and is therefore larger for states of high energy (large l) having a smaller confinement; the other involves intraband or interband transitions in the same layer. Then in the case of χ_A the coefficient $b^{(l)}$ is expected to be related to the "two-photon" density of states, but also to have a magnitude increasing with the index l . The transitions between confined and unconfined states have recently been investigated, showing that the corresponding probabilities are not at all negligible; therefore we believe that transitions such as those depicted in Fig. 1(a) can make a relevant contribution to the second-order susceptibility. We note that tensor χ_A (and χ_B) exhibits the symmetry properties of bulk materials rather than those of χ_C , as the considerations applicable to the latter one^{1,2} no longer hold.

In conclusion, the components of the a and b tensors, appearing in the phenomenological expression (2), are complex and frequency dependent; a takes into account the contribution of the non-resonant states, while b involves the one-photon resonant transitions, as evidenced by the resonant denominator in (2). For photon energies near those of the indirect band gap, the one-photon resonances are connected to the tensors χ_A and χ_C . The terms related to tensor b contain, as shown in (4), the product of three dipole matrix elements between electronic states: one matrix element refers to the resonant transition l ; the two others refer to transitions involving only confined states for χ_C , but for χ_A to transitions between confined and unconfined states. As these tensors obey different symmetry selection rules, their respective contributions and weights can be measured with a proper choice of polarization configuration.

EXPERIMENT

Measurements have been performed on InP bulk samples and InP/Al_{1-x}In_xAs heterostructures consisting of 50 periods of alternating layers of 40-Å InP and 100-Å Al_{0.48}In_{0.52}As deposited on a 500- μ m-thick substrate of InP. The InP cap layer has been removed by chemical etching, and the rear surface of the substrate optically polished. The samples have typical dimensions of 4×4 mm² and crystal axes directed along the diagonals. We have performed two sets of measurements on several samples at room temperature and at 10 K in a reflection geometry; in this way, due to the strong absorption of the

second-harmonic beam, the unwanted contribution from the InP substrate of the heterostructure is eliminated.

In the experimental setup for the study of second-harmonic generation, the principal source is a nanosecond Nd:YAG (yttrium aluminum garnet) laser, with injection seeding, at a repetition rate of 10 Hz (Quantel YG 580), pumping with its second harmonic a dye laser (Quantel TDL 50); its wavelength was tuned in the range 625–740 nm using DCM, LDS 698, and LDS 722 dyes. The working wavelengths, in the range 844–1069 nm (1.47–1.16 eV), were obtained by a Raman shifter filled with gaseous H₂ (Quantel RDS1) delivering pulses of a few mJ with a spectral width of ~ 0.4 meV. The IR beam, from the Raman shifter, after spectral filtering and attenuation, is split in two parts and sent to two similar apparatuses. In each of them, after passing through achromatic Fresnel rhombs and Glan-laser prisms for proper polarization selection, the beam is tightly focused on the sample with a spot of ~ 0.03 mm². The beams impinge on the samples at the settled angle θ with respect to the surface normal; the second-harmonic radiation, produced in the reflection direction, is collected by a lens and, after polarization filtering, sent to a double monochromator; the transmitted photons are detected by a photomultiplier and its signal sent to a gated integrator synchronized with the laser pulses. The outputs of the two systems, after digital conversion, are collected by a personal computer (PC) which provides control of the spectrometers and proper normalization of the signals. The first of the two apparatuses is used for the study of the sample under investigation, the second for generation and detection of the second harmonic on a reference sample consisting of a platelet of bulk GaAs. The signal produced by the GaAs crystal is used for the normalization of the signal generated by the sample under study. This procedure, with an identical excitation and detection geometry for both samples, minimizes the effects of the noise and instabilities of the Raman-shifted beam due to the stimulated process of generation of the IR radiation. GaAs has been preferred to other reference materials (e.g., quartz) because it has characteristics similar to those of InP, and, in the spanned frequency range, a relatively flat dispersion of the second-harmonic coefficient;^{21,24} its use has indeed proved advantageous for an accurate normalization of the data. The efficiencies of the two detection apparatuses have been measured using a calibration lamp; their ratio has been compared with that obtained by placing, on both branches, two GaAs samples in the same configuration, and a good agreement between the two was obtained.

RESULTS

The dependence of the signal at 2ω on the square of the intensity I_1 of the beam at the fundamental frequency ω has been tested varying I_1 over a decade, and turns out to be very well satisfied in the spanned range of energies for all tested samples. In order to check the symmetry properties of the $\chi^{(2)}$ tensor for the heterostructure, we have analyzed the dependence of the second-harmonic intensity on the polarization of the incoming beams, the crystal

axes orientation (specified by the angle α between the x direction and a crystallographic axis), and the incidence angle. Measurements have been performed at several energies of the incident photon at room temperature. The search for a signal coming from the elements χ_{zxz} , χ_{zxx} , χ_{zzz} , or equivalent has been done in a configuration with $\alpha=0$ and both the polarization directions of the incident beam and the analyzer perpendicular or parallel to the incidence plane ($\varphi=0$ or $\varphi=\pi/2$, respectively); no signal has been observed in these configurations. The signal-to-noise ratio, in the polarization configuration allowed, is of the order of 100; thus we can argue that these elements of $\chi^{(2)}$ for the heterostructure are at least one order of magnitude smaller than the element χ_{xyz} . In addition, we find that $\chi_{zxy}=\chi_{xyz}$ within an error of $\pm 10\%$. The theoretical calculations reported in Ref. 6 for an AlAs/GaAs heterostructure give a difference between these two tensor elements that is lower than 10%. In conclusion, from all these measurements, the dependence of the second-harmonic intensity on the various angles is in good agreement with that expected for $\chi^{(2)}$ for a crystal with symmetry T_d . We did not find, within the experimental errors, any evidence of contributions deriving from elements of $\chi^{(2)}$ related to a lower symmetry (e.g., D_{2d} or C_{2v}).

The second-harmonic spectra in the range 1.15–1.45 eV for both InP and the heterostructure have been measured at 10 and 300 K in a configuration with $\alpha=0$ and $\varphi=\pi/2$. The spectra for the heterostructure and the InP substrate, normalized to that of GaAs, are shown in Fig. 2. A clear enhancement of the second-harmonic signal of the heterostructure, compared to that of bulk InP, is observed at energies larger than 1.2 eV. In Fig. 3(a) we report the dispersion of $|\chi^{(2)}|$ derived from the above spec-

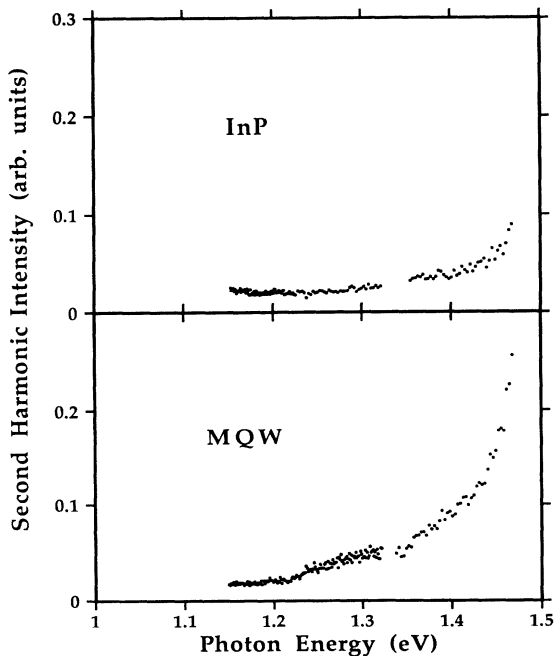


FIG. 2. The second harmonic intensity, relative to GaAs, for InP and the MQW. In the abscissa the energy of the photon at the fundamental frequency is reported.

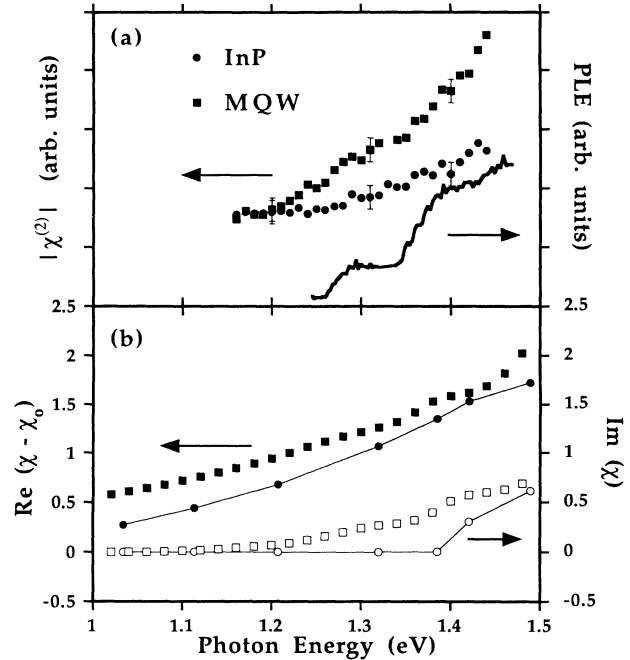


FIG. 3. (a) Modulus of the second-order susceptibility derived from the spectra of Fig. 2 for InP (circles) and the MQW (squares). Also shown is the PLE spectrum of the MQW (continuous line). (b) The real (full) and imaginary (empty) parts of the linear susceptibility χ at 300 K for InP (circles) and the MQW (squares). For the latter the values are calculated, and χ_0 is the electronic susceptibility at $\omega=0$. For InP the values are taken from Refs. 25 and 26, and we have assumed $\chi_0=10.0$.

tra after their reduction with the second-harmonic efficiency of GaAs,^{21,24} the efficiency of the detection apparatus and the numerical factor related to the refractive indices n_i and absorbances k_i appearing in (4). For InP, n and k have been derived from Refs. 25 and 26; for the heterostructure the corresponding values around 2ω have been assumed to be equal to those of InP, lacking any information about them, and those around the fundamental frequency ω derived from recent measurements.²⁷ Also shown in the same figure is the photoluminescence excitation spectrum (PLE) of the heterostructure, at 10 K, obtained by detection of the luminescence at 1.22 eV and exciting with the same nanosecond pulses used for the second harmonic spectra. For the heterostructure the spectrum of $\chi^{(2)}$ can be compared with that of the linear susceptibility. In Fig. 3(b) we show the dispersion of $\text{Im}\chi$ calculated on the basis of the theory developed in Ref. 17, and using the value of the transition dipole moment as a free parameter for the matching of the measured absorption coefficient. The calculated absorption spectrum is in good agreement with the measured excitation spectra reported in Fig. 3(a) and elsewhere.^{15,27} In the same figure we also show $\text{Re}\chi$ calculated, up to an additive constant, through Kramers-Krönig relations. From the comparison of χ and $\chi^{(2)}$ it appears that the latter has an enhancement that is coincident with the indirect band-to-band transitions of the MQW. We note, by the way, that exciton states relative to the spatially indirect transitions have not been detected in these MQW's, and that direct transitions in the InP and $\text{Al}_{1-x}\text{In}_x\text{As}$ layers fall,

at 10 K, at 1.51 and 1.62 eV, respectively. Thus the observed increase in the second-harmonic generation can reasonably be ascribed to band-to-band transitions between electron- and hole-confined states. At high energy the steepest dispersion, with respect to that of χ , shows that enhancement factors deriving from “two-photon resonances” or others must be taken into account. In Fig. 3(b) the dependence of the real and imaginary parts of the linear susceptibility for InP are shown for comparison.

Other useful information can be obtained from the dependence of the second-harmonic spectra on the temperature and band filling. As far as temperature is concerned, no significant variations of the second-harmonic spectra and efficiency have been observed between 10 and 300 K in both InP and the MQW. A possible effect of band filling on second-harmonic efficiency has been investigated by sending over the sample, in spatial and temporal superposition with the IR beam at frequency ω , a pump beam at 532 nm. In this way a significant band-filling effect over a wide range (~ 100 meV) can be produced, and has been observed in both luminescence and excitation spectra.²⁷ In these conditions the induced variations for the second-harmonic generation are found to be lower than a few percent, which corresponds to the noise level in the experiment. Hence the observed behavior is similar to that of the real part of χ , for which the temperature and band filling induce only minor changes of a few percent or less. In other words, in this frequency region the main contribution to $\chi^{(2)}$ from “one-photon” transitions comes from the virtual ones between levels with an energy difference much larger than $\hbar\omega$.

In conclusion, the observed enhancement of $\chi^{(2)}$ in the explored region is related to the continuum of states connected with the spatially indirect transitions of this type-II heterostructure, but it seems to result mainly from “two-photon” resonance effects rather than from the quantum confinement.

Finally, in order to quantify the magnitude of χ_{xyz} , the ratio between the second harmonic intensities of InP and GaAs has been measured: from our measurements at

$\hbar\omega = 1.2$ eV we find 1.3 ± 0.1 ; the spectra of Fig. 1 then directly gives the relative values of $|\chi^{(2)}|$ over the whole frequency range.

CONCLUSIONS

The second-harmonic spectra of InP and a type-II MQW of InP/Al_{1-x}In_xAs have been measured in the frequency region 1.15–1.45 eV, covering the range between the direct and spatially indirect band gaps. From a comparison of the data relative to the heterostructure and to InP, a contribution to the second-order susceptibility related to one-photon transitions between confined states belonging to different layers has been evidenced in the MQW. From a study of the symmetry properties of $\chi^{(2)}$, it has been possible to discriminate between the different contributions. The terms of $\chi^{(2)}$ deriving exclusively from transitions between confined states, which dominate the second-harmonic generation in the IR, in this case seem negligible in comparison to those also involving transitions with states into the continuum; therefore, according to theoretical calculations reported in Ref. 6, $\chi^{(2)}$ exhibits full symmetry of the class T_d or D_{2d} . As in the case of the bulk semiconductors, the main contribution to the dispersion of $\chi^{(2)}$ around the gap comes from the dispersion of the two-photon resonant terms which, presumably, is responsible for the enhancement observed in the MQW with respect to InP. Therefore these results show that the theoretical calculations of $\chi^{(2)}$, for second-harmonic generation in the visible, must take into account in an essential way transitions with the unconfined states lying at higher energy. The observed enhancement of the second-harmonic efficiency does not seem related to the confinement; however, a significant contribution from confinement can be expected for samples of better quality, where excitonic states should play a major role.²⁸ The samples investigated show, near the indirect band gap, an efficient second-harmonic generation with a negligible absorption of the fundamental beam; an improvement of the performances can be obtained in the future by a proper engineering of the MQW bands.¹⁰

¹J. Khurgin, Phys. Rev. B **38**, 4056 (1988).

²Leung Tsang *et al.*, Phys. Rev. B **41**, 5942 (1990).

³E. Rosencher, P. Bois, J. Neagle, E. Constard, and D. Delaire, Appl. Phys. Lett. **55**, 1597 (1989).

⁴E. Rosencher, P. Bois, J. Neagle, E. Constard, and D. Delaire, Superlatt. Microstruct. **8**, 369 (1990).

⁵P. J. Harshman and S. Wang, Appl. Phys. Lett. **60**, 1277 (1992).

⁶Ed Ghahramani, D. J. Moss, and J. E. Sipe, Phys. Rev. B **43**, 9269 (1991).

⁷Tz. Lue, K. Y. Lo, and C. C. Tzeng, IEEE J. Quantum Electron. **QE-28**, 302 (1992).

⁸Y. L. Xie *et al.*, Phys. Rev. B **43**, 12 477 (1991).

⁹C. Sirtori, F. Capasso, D. L. Sivco, A. L. Hutchinson, and A. Cho, Appl. Phys. Lett. **60**, 151 (1992).

¹⁰S. Scandolo, A. Baldereschi, and F. Capasso, Appl. Phys. Lett. **62**, 3138 (1993).

¹¹A. Shimizu, Phys. Rev. Lett. **61**, 613 (1988).

¹²G. R. Olbright *et al.*, Phys. Rev. B **44**, 3043 (1991).

¹³J. Bleuse, P. Voisin, M. Voos, H. Munekata, L. L. Chang, and L. Esaki, Appl. Phys. Lett. **52**, 462 (1988).

¹⁴J. A. Brum, P. Voisin, and G. Bastard, Phys. Rev. B **33**, 1063 (1986).

¹⁵E. Lugagne-Delpon, P. Voisin, J. P. Vieren, M. Voos, J. P. André, and J. N. Patillon, Semicond. Sci. Technol. **7**, 524 (1992).

¹⁶E. Lugagne-Delpon, P. Voisin, M. Voos, and J. P. André, Appl. Phys. Lett. **60**, 3087 (1992).

¹⁷P. Voisin, G. Bastard, and M. Voos, Phys. Rev. B **33**, 1063 (1986).

¹⁸A. Stahl and I. Balslev, *Electrodynamics of the Semiconductor Band-edge* (Springer, Berlin, 1987).

¹⁹Y. Shen, *The Principles of Nonlinear Optics* (Wiley, New York, 1984).

²⁰C. Flytzanis, in *Quantum Electronics*, edited by H. Rabin and C. L. Tang (Academic, New York, 1975), Vol. 1.

²¹D. Bethune, A. J. Schmidt, and Y. R. Shen, Phys. Rev. B **11**,

- 3867 (1975).
- ²²D. J. Moss, J. E. Sipe, and H. M. van Driel, *Phys. Rev. B* **36**, 9708 (1987).
- ²³M. Z. Huang and W. Y. Ching, *Phys. Rev. B* **47**, 9464 (1993).
- ²⁴H. Lotem, G. Koren, and Y. Yacoby, *Phys. Rev. B* **9**, 3532 (1974).
- ²⁵B. O. Seraphin and H. E. Bennett, in *Semiconductors and Semimetals*, edited by R. K. Willardson and A. C. Beer (Academic, New York, 1967), Vol. 3.
- ²⁶H. Burkhard, H. W. Dinges, and E. Kuphal, *J. Appl. Phys.* **53**, 655 (1982).
- ²⁷S. Cioncolini, Ph.D. thesis, University of Florence, Florence, 1992.
- ²⁸M. Matsuura and Y. Shinozuka, *Phys. Rev. B* **38**, 9830 (1988).